Journal of Molecular Medicine
https://doi.org/10.1007/s00109-023-02318-3

ORIGINAL ARTICLE

TRIM-containing 44 aggravates cardiac hypertrophy via TLR4/NOX4-induced ferroptosis

Leiming Wu[1] · Meng Jia[2] · Lili Xiao[1] · Zheng Wang[1] · Rui Yao[1] · Yanzhou Zhang[1] · Lu Gao[1]

Received: 10 November 2022 / Revised: 1 April 2023 / Accepted: 11 April 2023

Abstract

TRIM-containing 44 (TRIM44) is a promoter of multiple cancers. However, its role in cardiac hypertrophy has not been elucidated. This study explored the role of TRIM44 on pressure overload-induced cardiac hypertrophy in mice. Mice were subjected to aortic banding to establish an adverse cardiac hypertrophy model, followed by the administration of AAV9-TRIM44 or AAV9shTRIM44 to overexpress or knock down TRIM44. Echocardiography was used to assess cardiac function. H9c2 cells were cultured and transfected with either Ad-TRIM44 or TRIM44 siRNA to overexpress or silence TRIM44. Cells were also stimulated with angiotensin II to establish a cardiomyocyte hypertrophy model. Results indicated that TRIM44 was downregulated in mice hearts and cardiomyocytes that were treated with aortic banding or angiotensin II. TRIM44 overexpression in mice hearts aggravated cardiac hypertrophy and fibrosis, as well as inhibited cardiac function post-aortic banding. Moreover, mice with TRIM44 overexpression displayed increased ferroptosis post-aortic banding. Mice with TRIM44 knockdown revealed ameliorated cardiac hypertrophy, ferroptosis, and fibrosis, as well as improved cardiac function post-aortic banding. In H9c2 cells transfected with Ad-TRIM44, angiotensin II-induced ferroptosis was enhanced, while cells with silenced TRIM44 reported reduced ferroptosis post-angiotensin II administration. Furthermore, TRIM44 interacted with TLR4, which increased the expression of NOX4 and subsequently augmented ferroptosis-associated protein levels. By using TLR4 knockout mice, the inhibitory role of TRIM44 was reduced post-aortic banding. Taken together, TRIM44 aggravated pressure overload-induced cardiac hypertrophy via increased TLR4/NOX4-associated ferroptosis.

Key messages

- TRIM44 could aggregate pressure overload-induced cardiac hypertrophy via increasing TLR4-NOX4 associated ferroptosis.
- Target TRIM44 may become a new therapeutic method for preventing or treating pressure overload-induced cardiac hypertrophy.

Keywords Pressure overload · TRIM44 · Cardiac hypertrophy · Ferroptosis · TLR4 · NOX4

Introduction

The heart functions to maintain blood perfusion throughout the entire body. When the pressure behind the ventricle increases, the heart and myocardial cells become hypertrophic, which increases the contractility of the myocardium [1]. Cardiac hypertrophy is accompanied by changes in myocardial quality and gene expression, thereby altering myocardial metabolism, myocardial cell survival, and myocardial contractility [2, 3]. Pathological myocardial hypertrophy is accompanied by adverse cardiovascular events, including heart failure, arrhythmia, and death [3]. At present, studies have confirmed that mechanical stretching, oxidative stress, and inflammatory response are the molecular bases

Leiming Wu and Meng Jia contributeequally.

✉ Yanzhou Zhang
yzzhang6@163.com

✉ Lu Gao
gaomei1215@163.com

[1] Department of Cardiology, the First Affiliated Hospital of Zhengzhou University, No.1 Jianshe East Road, Zhengzhou 450052, China

[2] Department of Thyroid Surgery, The First Affiliated Hospital of Zhengzhou University, Zhengzhou, China

Published online: 29 April 2023

of pathological hypertrophy in cardiomyocytes [4, 5]. Furthermore, there is no effective pharmacological intervention approved for cardiac hypertrophy. Therefore, the identification of therapeutic targets for myocardial hypertrophy is essential for the prevention and treatment of heart failure.

Tripartite motif (TRIM) family members are conservative factors containing RING finger, B-box, and coiled-coil (RBCC) domains [1, 6]. Previous studies have found that multiple TRIM family members are closely related to a variety of cardiovascular diseases, such as heart development, autophagy regulation, and cardiomyopathy [7, 8]. TRIM44 is a member of the TRIM family and is mainly involved in immune response, tumorigenesis, and development [9, 10]. Recently, TRIM44 was reported to participate in hypoxia-induced cardiomyocyte injury [10, 11]. Luo et al. reported that a non-coding RNA hypoxia-inducible factor-1α (HIF1A)-antisense RNA 2 (HIF1A-AS2) suppressed TRIM44 to protect cardiomyocytes against hypoxia-induced injury [11]. Based on these studies, we hypothesized that TRIM44 might participate in the progression of pressure overload-induced cardiac hypertrophy. In this study, the role of TRIM44 on adverse cardiac hypertrophy was explored, where AAV9-TRIM44 or AAV9-shTRIM44 were used to overexpress or knock down TRIM44 in mice hearts.

Materials and methods

Animals

C57BL/6 J male mice (23.5–27.5 g) of 8–10 weeks were purchased from the Chinese Academy of Medical Sciences & Peking Union Medical College. The animal experiments were performed according to the Guide for the Care and Use of Laboratory Animals published by the US National Institutes of Health (NIH Publication No. 85–23, revised 1996) and were approved by the Animal Care and Use Committee of the First Affiliated Hospital of Zhengzhou University (ZH-2021–0120). Each mouse was subjected to aortic banding (AB). One week before AB surgery, mice were subjected to injection of AAV9, harboring TRIM44 or shTRIM44 (60 µl, $5.0–6.5 \times 10^{13}$ GC/ml), via retroorbital venous. To understand its mechanism, TLR4 knockout (KO) mice, purchased from Jackson Lab, were subjected to AB surgery and AAV9-TRIM44 injection ($n = 12$). All experiments in the study were performed as blinded experiments.

Animal model

The mice were anesthetized by intraperitoneal injection of 3% pentobarbital sodium. The mice were then intubated, and the skin between the third and fourth left ribs of the mouse sternum was opened. The thoracic aorta was exposed, and a 7/0 surgical suture was used to cross the aorta. At the same time, a 27G needle was placed parallel to the main artery, and the aorta was ligated. In the sham group, the thread was hung without ligation. The thoracic cavity and skin of the mice were sutured, and the mice were injected with temgesic (0.1 mg/kg) once a day for 6 days. The cardiac function of mice was evaluated by echocardiography 4 weeks after the AB operation.

AAV9 construction and viral delivery

Viral vectors (AAV9-TRIM44 and AAV9-shTRIM44) and troponin T were purchased from Vigene Bioscience Company (Jinan, China). One week before AB surgery, the mice were randomly assigned to receive either 60–80 µl AAV9-TRIM44 or AAV9-shTRIM44 at $5.0–6.5 \times 10^{13}$ GC/ml in sterile PBS at 37 °C by injection into the retroorbital venous plexus, as described in a previous study [12].

Echocardiography measurements

Mylab30CV (ESAOTE) echocardiography was used to detect cardiac function. Both M-mode and pulse Doppler were recorded with a 15 MHz probe. The left ventricular ejection fraction (LVEF) and left ventricular shortening fraction (LVFS) were calculated.

Histological analysis

Heart tissues were removed and fixed in 10% formalin, then embedded in paraffin and cut into 25-µm sections. Hematoxylin and eosin (H&E) staining was performed, and a digital camera (Olympus BX 53 microscope, Tokyo, Japan) was used for observation.

Fe assays and malondialdehyde (MDA) level

Non-heme iron levels in serum and heart tissue were determined with the Fe assay kit (ab83366, Abcam), as per the operational guidelines. In short, tissues were rinsed in chilled PBS before homogenization on ice in Fe assay buffer with a Dounce homogenizer, followed by centrifugation at $16,000 \times g$ for 10 min. The supernatant of the Fe assay was then collected, and the samples were diluted with assay buffer to a final volume of 100 µl. The sample was then incubated with 5-µl Fe reducer (for total Fe) or assay buffer (for ferrous Fe) along with standards at 37 °C for 30 min. In each well, 100 µl of Fe probe was added and mixed, followed by incubation at 37 °C in the dark for 1 h. Absorbance was measured at 593 nm with a microplate reader. Fe levels were calculated according to the standard curve and normalized to protein levels from the Bradford protein assay.

MDA level was determined from a commercial kit (Beyotime, Bio., Shanghai, China). Absorbance was measured at 532 nm with a microplate reader.

Cell culture

Rat cardiomyocytes H9c2 (Cell Bank of the Chinese Academy of Sciences, Shanghai, China) were grown in DMEM (C11995; Gibco, Grand Island, NY, USA), supplemented with 10% FBS, penicillin (100 U/ml), and streptomycin (100 mg/ml) (Gibco), in a humidified CO_2 incubator (SANYO 18 M, Osaka, Japan) with 5% CO_2 at 37 °C. Cells were incubated with LPS (1 μg/ml) for 12 h to establish a cell injury model or stimulated with Ang II (1 μM) for 48 h to induce cardiomyocytes hypertrophic model. Cells were transfected with Ad-TRIM44 or TRIM44 siRNA to overexpress or silence TRIM44. Cell viability was determined by MTT assay (Beyotime, Bio., Shanghai, China).

Detection of reactive oxygen species

Adherent H9c2 cardiomyocytes were digested with 0.25% trypsin and centrifuged for 5 min. The cells were counted and resuspended in phosphate buffer. H9c2 cells were incubated with 2′, 7′-dichlorofluorescein diacetate (DCFH-DA) fluorescent probes for 20 min. The fluorescence intensity in each sample was measured by flow cytometry (Beckman, USA).

Detection of lipid reactive oxygen species

After treatment, cells were incubated with 5-μl C11-BODIPY fluorescence probes for 40 min, and the fluorescence intensity of each group was measured by a microplate reader (Synergy HT, BioTek, Vermont, USA).

Nicotinamide adenine dinucleotide phosphate (NADPH) oxidase in cardiomyocytes was detected using commercial kits from Beyotime, Bio. (Shanghai, China), according to the manufacturer's instructions.

Prussian blue staining

Heart slices were dewaxed at 60 °C, followed by hydration of the heart in distilled water. The preparation of the dyeing solution involved mixing equal volumes of potassium ferrocyanide solution and hydrochloric acid. Heart sections were incubated in the staining solution for 3 min. Photographs were taken with a light microscope (Olympic, Japan).

RT-PCR and western blot

TRIzol reagent was used to isolate total mRNA. Smart SpecPlus Spectrophotometer (Bio-Rad) was used to detect mRNA purity with OD260/OD280 ratios. A total of 2 μg of mRNA was reverse transcribed into cDNA with a cDNA Synthesis Kit (Roche Diagnostics). The Light Cycler 480 SYBR Green I Master Kit (Roche Diagnostics) was used for amplifications, with GAPDH as a reference.

For western blotting, radioimmunoprecipitation (RIPA) lysis buffer was used to lyse cells. Total protein concentration was measured by the BCA method and then loaded onto SDS-PAGE. When proteins were transferred to polyvinylidene difluoride (PVDF) membranes (Millipore), they were incubated with primary antibodies at 4 °C overnight. Primary antibodies including TRIM44, TLR4, NOX4, ferritin, Gpx4, and GAPDH were purchased from Abcam (1:100 dilution, Hercules, CA, USA). Blots were developed with enhanced chemiluminescence (ECL) reagents (Bio-Rad, Hercules, CA, USA) and visualized by a ChemiDoc MP Imaging System (Bio-Rad). GAPDH was used as a reference.

Co-IP assay

For immunoprecipitation, 10 μl protein A/G-agarose beads and 1 μg antibody were incubated with each sample (500 μl) overnight at 4 °C. After washing with immunoprecipitation buffer, the eluted proteins were immunoblotted with the indicated primary antibodies.

Data analysis

All data were expressed as mean ± SD. SPSS 23.3 was used for data analysis. Shapiro–Wilk test was used to test the normality distribution of data; all the data were normally distributed. Student's t-test was used to compare data between two groups. One-way ANOVA and two-way ANOVA, followed by Tukey's post hoc test, were used to compare data between more than two groups. p values less than 0.05 denoted statistical significance.

Results

The expression level of TRIM44 in hypertrophic heart

To explore the role of TRIM44 in adverse cardiac hypertrophy, mice were subjected to AB to establish a cardiac hypertrophy model. The expression level of TRIM44 was upregulated as compared to sham mice (Fig. 1A). TRIM44 expression was increased in cardiomyocytes with Ang II treatment (Fig. 1B).

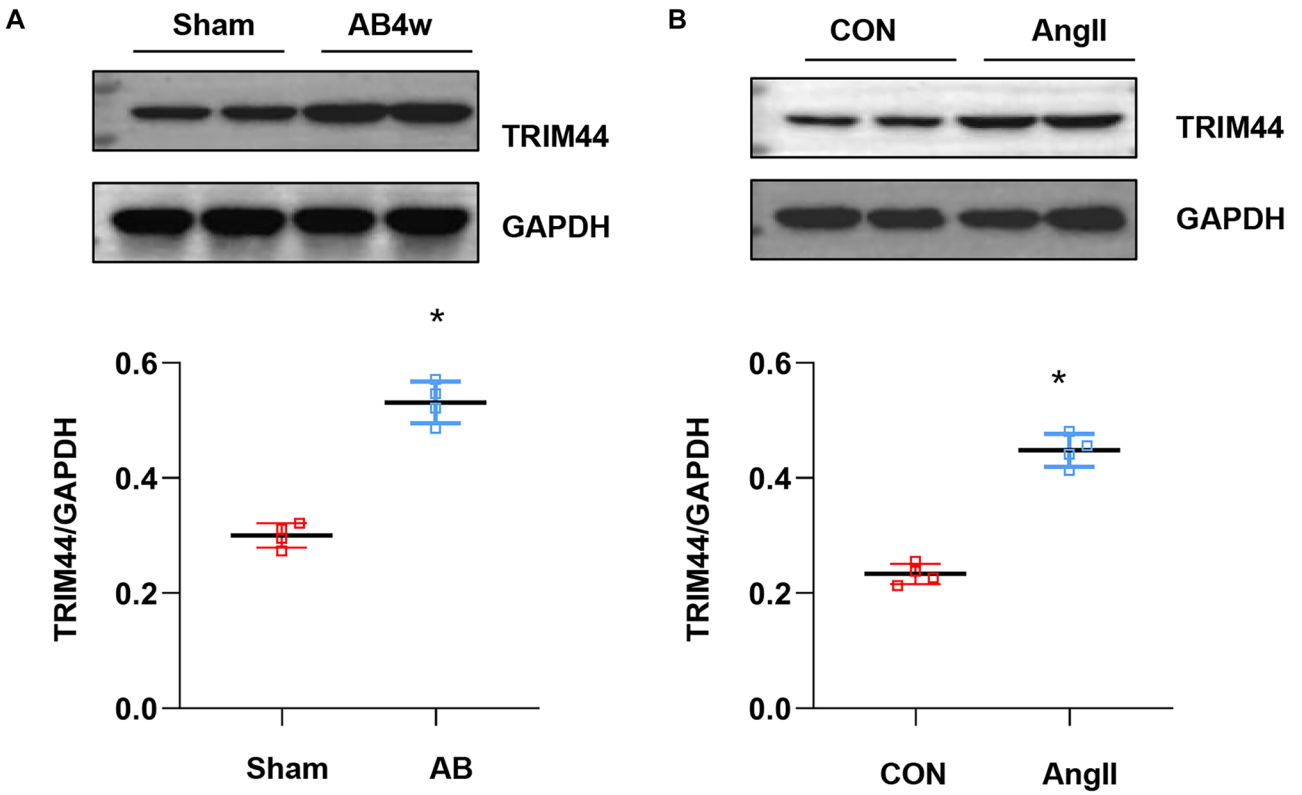

Fig. 1 The expression level of TRIM44 in hypertrophic heart. **A** Protein level of TRIM44 in mice hearts 4 weeks post-AB ($n=4$). **B** Protein level of TRIM44 in cardiomyocytes challenged with Ang II ($n=4$). *$p<0.05$ vs. CON group

TRIM44 overexpression in the heart aggravated cardiac hypertrophy, fibrosis, and cardiac dysfunction

The protein level of TRIM44 was upregulated after AAV9-TRIM44 injection (Fig. 2A). Four weeks post-AB, the heart weight to body weight ratio (HW/BW), the heart weight to tibia length ratio (HW/TL), and the lung weight to body weight ratio (LW/BW) increased, indicating lung edema (Fig. 2B). TRIM44 overexpression in the heart further increased these ratios (Fig. 2B). H&E staining displayed increased cross-sections in the AB group as compared with the sham group (Fig. 2C and D), which was enhanced by TRIM44 overexpression. The left ventricular (LV) end-diastolic diameter (LVEDD) and the LV end-systolic diameter (LVESD) increased in mice 4 weeks post-AB (Fig. 2E and Table 1). LV ejection fraction (LVEF) and LV fractional shortening (LVFS) drastically reduced in mice 4 weeks post-AB as compared to the sham group. Likewise, LVEDD and LVESD increased in the TRIM44 overexpression group, while both LVEF and LVFS decreased in the TRIM44 overexpression group as compared to the NC-AB group. The hypertrophic markers, such as ANP, BNP, β-MHC, and α-MHC, were also detected. The transcription of ANP, BNP, and β-MHC was upregulated, whereas α-MHC decreased in mice 4 weeks post-AB. TRIM44 overexpression further enhanced the mRNA levels of ANP, BNP, and β-MHC, and diminished the mRNA level of α-MHC (Fig. 2F). The fibrosis markers and pro-inflammatory factors were also assessed, where TRIM44 overexpression deteriorated pressure overload-induced fibrosis and inflammation (Fig. 2G and H).

TRIM44 overexpression in the heart enhanced ferroptosis

Lipid peroxidase was measured in mice hearts. The levels of MDA in serum and heart increased in mice 4 weeks post-AB (Fig. 3A and B). Likewise, TRIM44 overexpression increased the level of MDA in the serum and heart of mice post-AB. Non-heme iron levels in serum and heart tissues were measured to assess ferroptosis. As expected, the level of non-heme iron in serum and heart increased

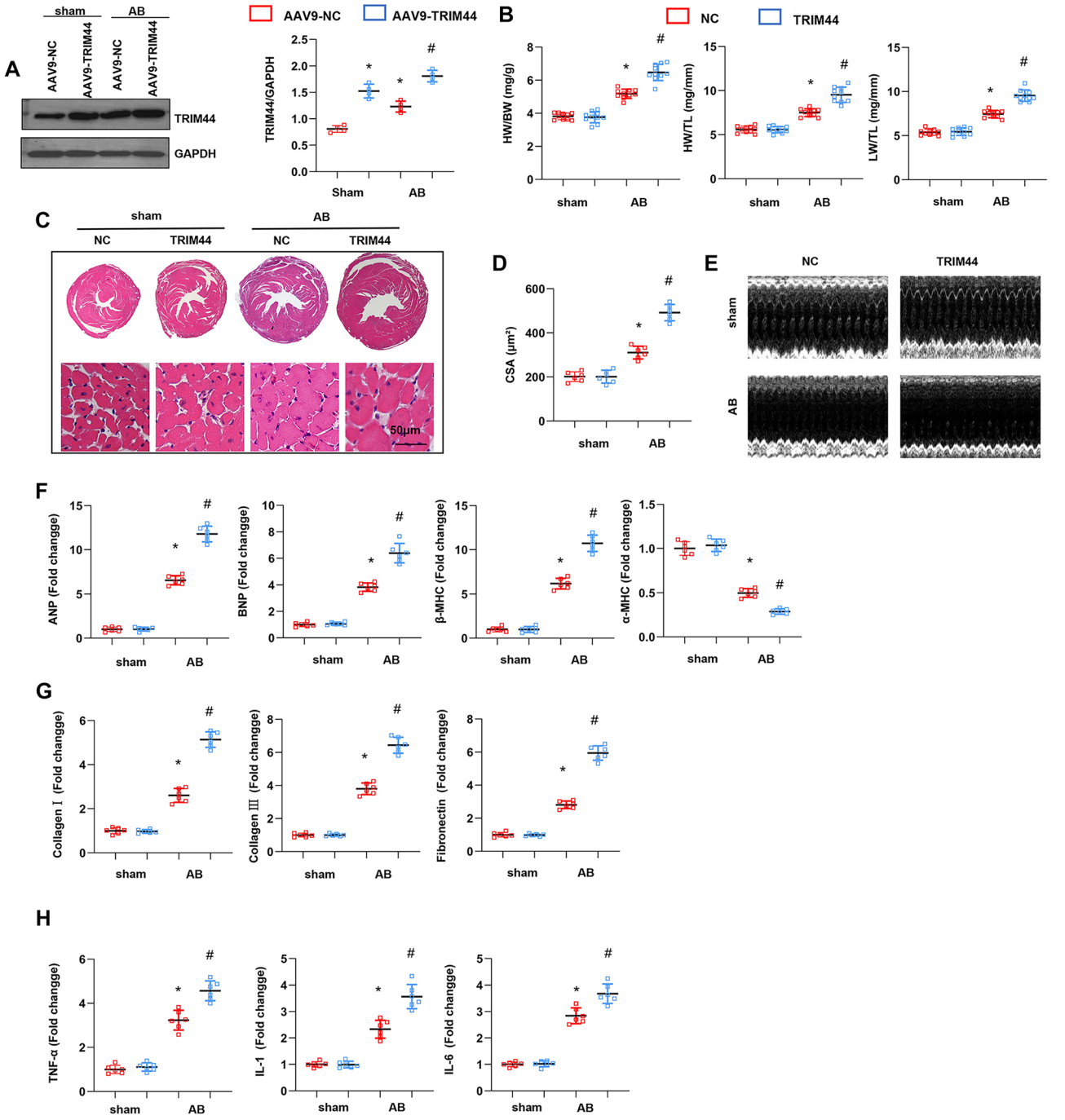

Fig. 2 TRIM44 overexpression in the heart-aggravated cardiac hypertrophy, fibrosis, and cardiac dysfunction. **A** Protein level of TRIM44 in AAV9-TRIM44 mice hearts ($n=4$). **B** Heart weight/body weight (HW/BW), HW/tibia length (HW/TL), and lung weight/BW (LW/BW) in mice hearts 4 weeks post-AB ($n=8$). **C**, **D** H&E staining of hearts in mice hearts 4 weeks post-AB ($n=6$). **E** Representative echocardiography images in each group. **F**, **G** mRNA levels of pro-hypertrophy and fibrosis markers in heart tissue 4 weeks post-AB ($n=6$). **H** mRNA levels of pro-inflammatory factors in heart tissue four weeks post-AB ($n=6$). *$p<0.05$ vs. NC/sham group. #$p<0.05$ vs. NC/AB group

in mice 4 weeks post-AB. TRIM44 overexpression also increased the level of non-heme iron in the serum and heart of mice post-AB (Fig. 3C and D). Iron staining displayed an increase in cardiac iron density in mice 4 weeks post-AB, which was further increased by TRIM44 overexpression (Fig. 3E and F).

Table 1 Echocardiography analysis in each group in mice with TRIM44 overexpression

Parameters	NC-Sham $n=6$	TRIM44-Sham $n=6$	NC-AB $n=6$	TRIM44-AB $n=6$
HR (min-1)	409.45 ± 33.24	410.63 ± 31.01	401.39 ± 23.21	412 ± 33.89
LVEDd (mm)	3.32 ± 0.23	3.26 ± 0.22	4.18 ± 0.30*	4.92 ± 0.30**
LVESd (mm)	2.61 ± 0.22	2.73 ± 0.22	3.20 ± 0.23*	3.90 ± 0.19**
LVEF (%)	72.63 ± 4.66	75.13 ± 4.88	54.75 ± 0.2.82*	31.50 ± 2.45**
LVFS (%)	36.63 ± 2.45	35.86 ± 2.03	27.00 ± 2.00*	19.25 ± 1.67**

HR heart rate, *LVEDd* left ventricular end diastolic dimension, *LVESd* LV end systolic dimension, *LVEF* left ventricular ejection fraction, *LVFS* left ventricular shortening fraction

*$p < 0.05$ for difference from corresponding sham group; **$p < 0.05$ vs AAV9-TRIM44-AB group

TRIM44 KO in the heart ameliorated cardiac hypertrophy, fibrosis, and cardiac dysfunction

TRIM44 KO mice were used to confirm the deteriorating role of TRIM44 on cardiac hypertrophy (Fig. 4A). The protein level of TRIM44 was sharply downregulated after AAV9-shTRIM44 injection. Four weeks post-AB, HW/BW, HW/TL, and LW/BW were increased, indicating lung edema (Fig. 4B). TRIM44 KO in the heart decreased these ratios (Fig. 4B). H&E staining found that the cross-sectional area was increased in the AB group when compared with the sham group (Fig. 4C and D), while TRIM44 KO diminished this change. Cardiac function was assessed by echocardiography (Fig. 4E and Table 2). LVEDD and LVESD were increased in mice 4 weeks post-AB. The LVEF and LVFS were sharply reduced in mice 4 weeks post-AB when compared with the sham group. LVEDD and LVESD were reduced in the TRIM44 KO group. LVEF and LVFS were enhanced in the TRIM44 KO group as compared to the scRNA-AB group. TRIM44 KO reduced the mRNA levels of ANP, BNP, and β-MHC, but increased the mRNA level of α-MHC (Fig. 4F). TRIM44 KO also attenuated pressure overload-induced fibrosis and inflammation (Fig. 4G and H).

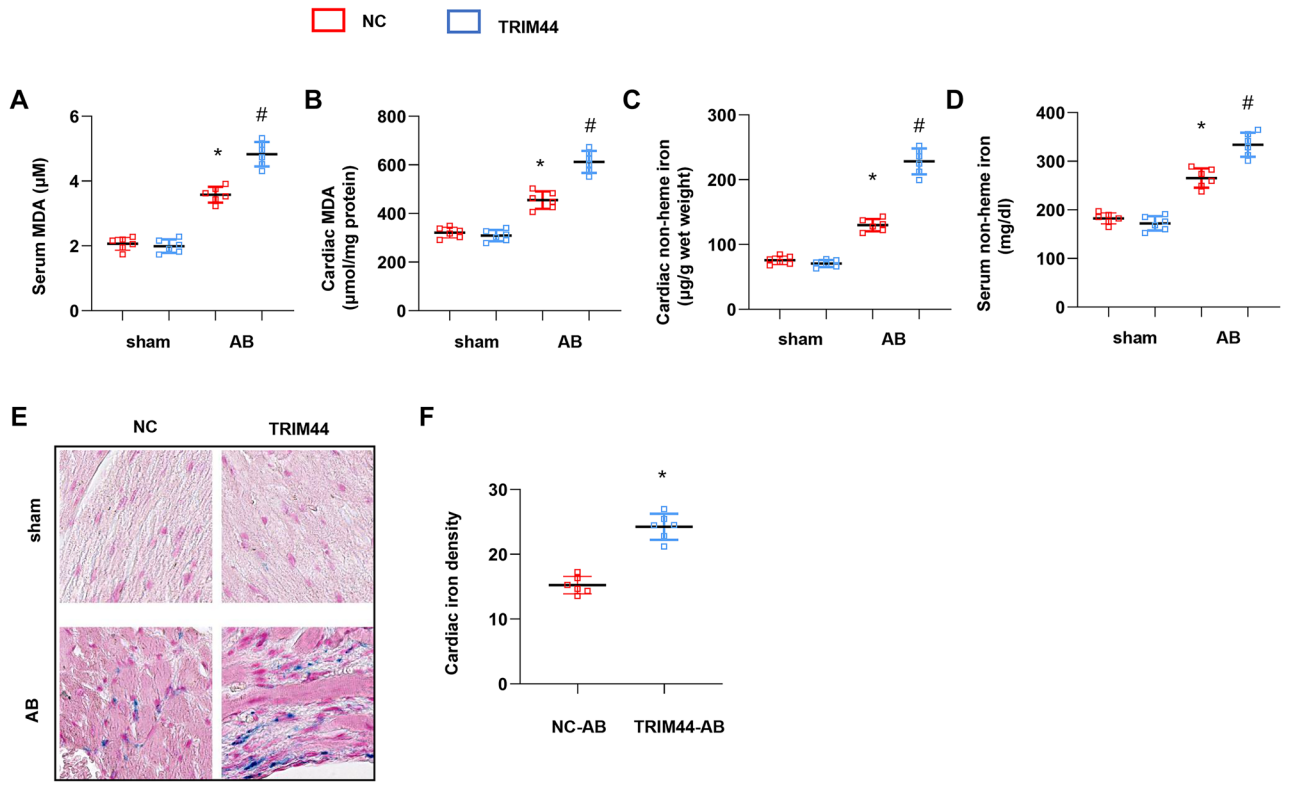

Fig. 3 TRIM44 overexpression in the heart-enhanced ferroptosis. **A**, **B** Serum and cardiac MDA levels in mice 4 weeks post-AB ($n=6$). **C**, **D** Serum and cardiac non-heme iron levels in mice 4 weeks post-AB ($n=6$). **E**, **F** Prussian blue staining and quantified results in AAV9-TRIM44 mice 4 weeks post-AB ($n=6$). *$p < 0.05$ vs. NC/sham group. #$p < 0.05$ vs. NC/AB group

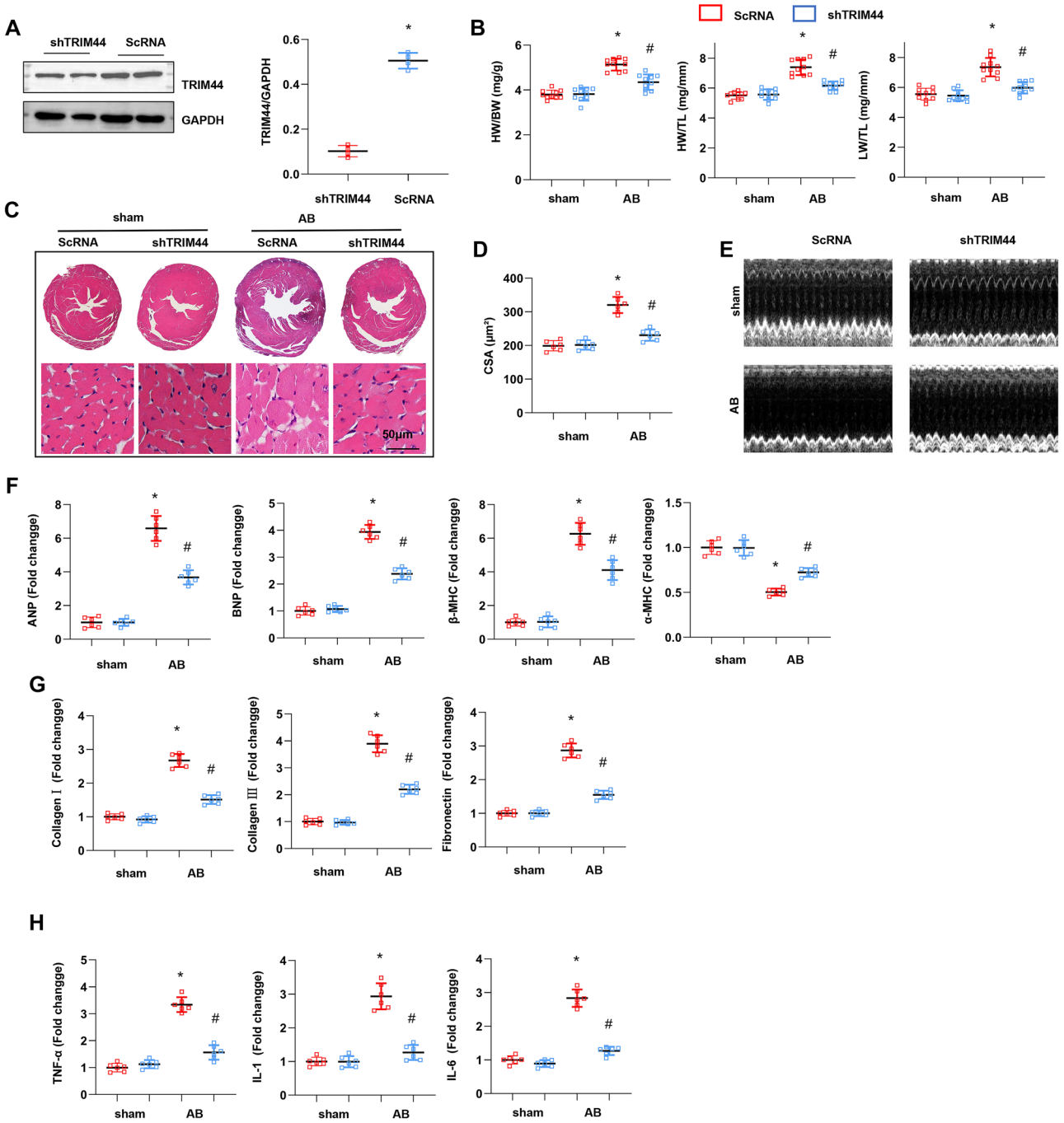

Fig. 4 TRIM44 knockdown in the heart-ameliorated cardiac hypertrophy, fibrosis, and cardiac dysfunction. **A** Protein level of TRIM44 in AAV9-shTRIM44 mice hearts ($n=4$). **B** HW/BW, HW/TL, and LW/BW in mice heart 4 weeks post-AB ($n=8$). **C**, **D** H&E staining of hearts in mice hearts 4 weeks post-AB ($n=6$). **E** Representative echocardiography images in each group. **F**, **G** mRNA levels of pro-hypertrophy and fibrosis markers in heart tissue 4 weeks post-AB ($n=6$). *$p<0.05$ vs. NC/sham group. #$p<0.05$ vs. NC/AB group. **H** mRNA levels of pro-inflammatory factors in heart tissue 4 weeks post-AB ($n=6$). *$p<0.05$ vs. scRNA/sham group. #$p<0.05$ vs. scRNA/AB group

TRIM44 KO in the heart inhibited ferroptosis

Lipid peroxidase was measured in the hearts of TRIM44 KO mice. The levels of MDA in serum and heart were increased in mice 4 weeks post-AB (Fig. 5A and B), while TRIM44 KO decreased the levels of MDA in the serum and heart of mice post-AB. Likewise, the level of non-heme iron in serum and heart increased in mice 4 weeks post-AB, while TRIM44 KO decreased the level of non-heme iron in the serum and heart of mice post-AB (Fig. 5C

Table 2 Echocardiography analysis in each group in mice with TRIM44 knockout

Parameters	ScRNA-Sham	shTRIM44-Sham	ScRNA-AB	shTRIM44-AB
HR (min-1)	419.10 ± 42.46	411.51 ± 43.38	407.27 ± 26.70	417.33 ± 39.76
LVEDd (mm)	3.23 ± 0.23	3.12 ± 0.21	4.23 ± 0.30*	3.58 ± 0.26**
LVESd (mm)	2.76 ± 0.21	2.60 ± 0.18	3.29 ± 0.20*	2.76 ± 0.16**
LVEF (%)	74.13 ± 4.70	74.38 ± 4.84	54.38 ± 4.07*	65.75 ± 3.88**
LVFS (%)	36.00 ± 2.00	36.5 ± 2.45	23.14 ± 2.03*	32.25 ± 2.12**

HR heart rate, *LVEDd* left ventricular end diastolic dimension, *LVESd* LV end systolic dimension, *LVEF* left ventricular ejection fraction, *LVFS* left ventricular shortening fraction

*$p < 0.05$ for difference from corresponding sham group; **$p < 0.05$ vs shTRIM44-AB group

and D). Iron staining displayed increased cardiac iron density in mice 4 weeks post-AB, while TRIM44 KO reduced cardiac iron density post-AB (Fig. 5E and F).

TRIM44 overexpression in cardiomyocytes increased cell ferroptosis

The protein level of TRIM44 was remarkably increased in cells transfected with Ad-TRIM44 (Fig. 6A). ROS and lipid ROS levels were sharply increased in cells stimulated with Ang II. Similarly, TRIM44 overexpression increased ROS and lipid ROS levels in cardiomyocytes treated with Ang II (Fig. 6B and C). MDA level and NADPH oxidase activity were also increased in the Ang II group. TRIM44 overexpression further increased MDA level and NADPH oxidase activity in cells treated with Ang II (Fig. 6D–G).

TRIM44 silence in cardiomyocytes suppresses cell ferroptosis

The protein level of TRIM44 was decreased in cells transfected with TRIM44 siRNA (Fig. 7A). ROS and lipid ROS levels were increased in cells stimulated with Ang II, while TRIM44 KO decreased ROS and lipid ROS levels

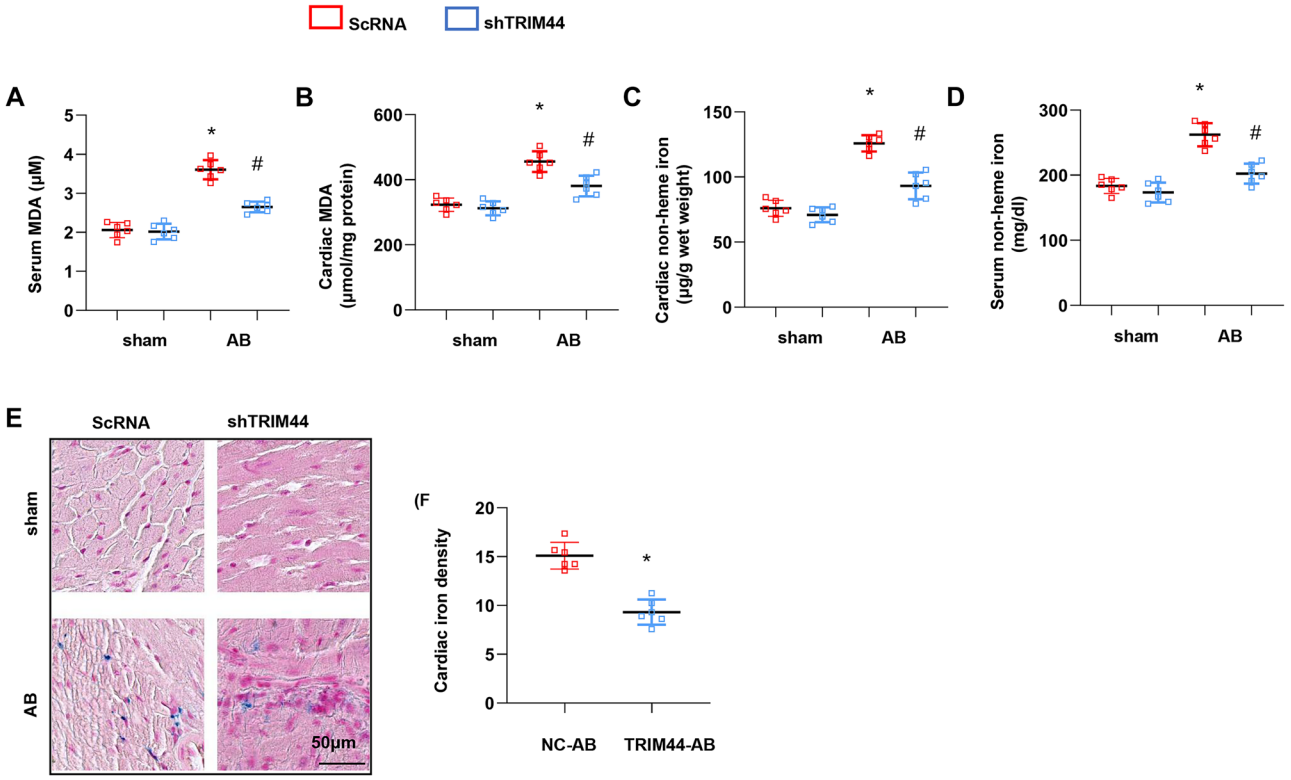

Fig. 5 TRIM44 knockdown in the heart-inhibited ferroptosis. **A**, **B** Serum and cardiac MDA levels in mice 4 weeks post-AB ($n = 6$). **C**, **D** Serum and cardiac non-heme iron levels in mice 4 weeks post-AB ($n = 6$). **E**, **F** Prussian blue staining and quantified results in AAV9-shTRIM44 mice 4 weeks post-AB ($n = 6$). *$p < 0.05$ vs. NC/sham group. #$p < 0.05$ vs. NC/AB group. *$p < 0.05$ vs. scRNA/sham group. #$p < 0.05$ vs. scRNA/AB group

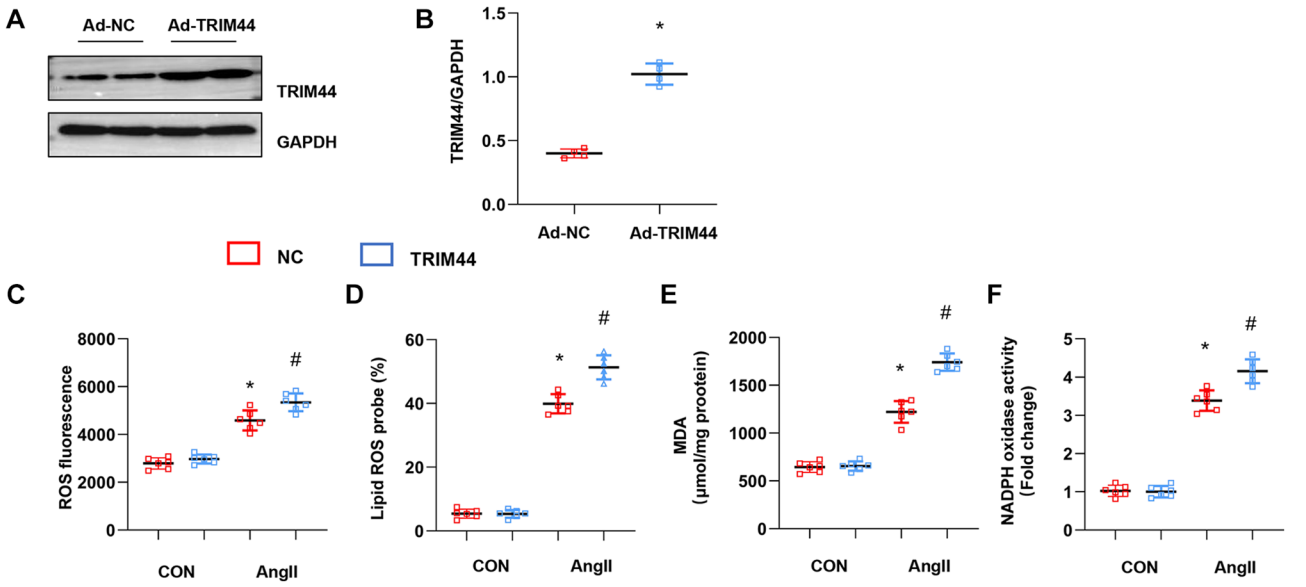

Fig. 6 TRIM44 overexpression in cardiomyocytes increased cell ferroptosis. H9c2 cells were transfected with Ad-TRIM44. **A**, **B** Protein levels of TRIM44 in Ad-TRIM44-transfected H9c2 cells ($n=4$). **C** ROS levels in H9c2 cells in each group ($n=6$). **D** Lipid ROS levels in H9c2 cells in each group ($n=6$). **E**, **F** MDA level and NADPH oxidase activity in each group ($n=6$). *$p<0.05$ vs. Ad-NC/CON group. #$p<0.05$ vs. Ad-NC/Ang II group

in Ang II-treated cells (Fig. 7B and C). The MDA level and NADPH oxidase activity were also increased in the Ang II group. TRIM44 KO further increased MDA level and NADPH oxidase activity in cells treated with Ang II (Fig. 7D–G).

TRIM44 interaction with TLR4 affected NOX4 signaling

The level of the ferroptosis marker ferroportin was increased in mice hearts post-AB (Fig. 8A and B). On the other hand,

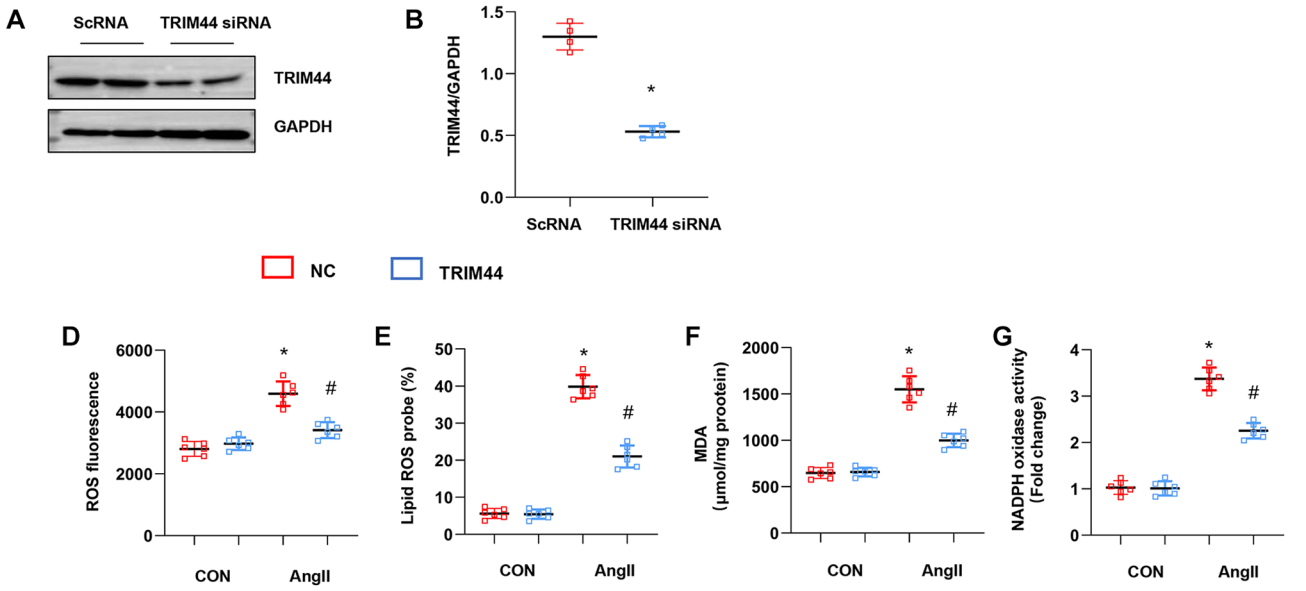

Fig. 7 TRIM44 silencing in cardiomyocytes suppressed cell ferroptosis. H9c2 cells were transfected with TRIM44 siRNA. **A**, **B** Protein levels of TRIM44 in Ad-TRIM44-transfected H9c2 cells ($n=4$). **C** ROS level in H9c2 cells in each group ($n=6$). **D** Lipid ROS level in H9c2 cells in each group ($n=6$). **E**, **F** MDA level and NADPH oxidase activity in each group ($n=6$). *$P<0.05$ vs. scRNA/CON group. #$P<0.05$ vs. scRNA/Ang II group

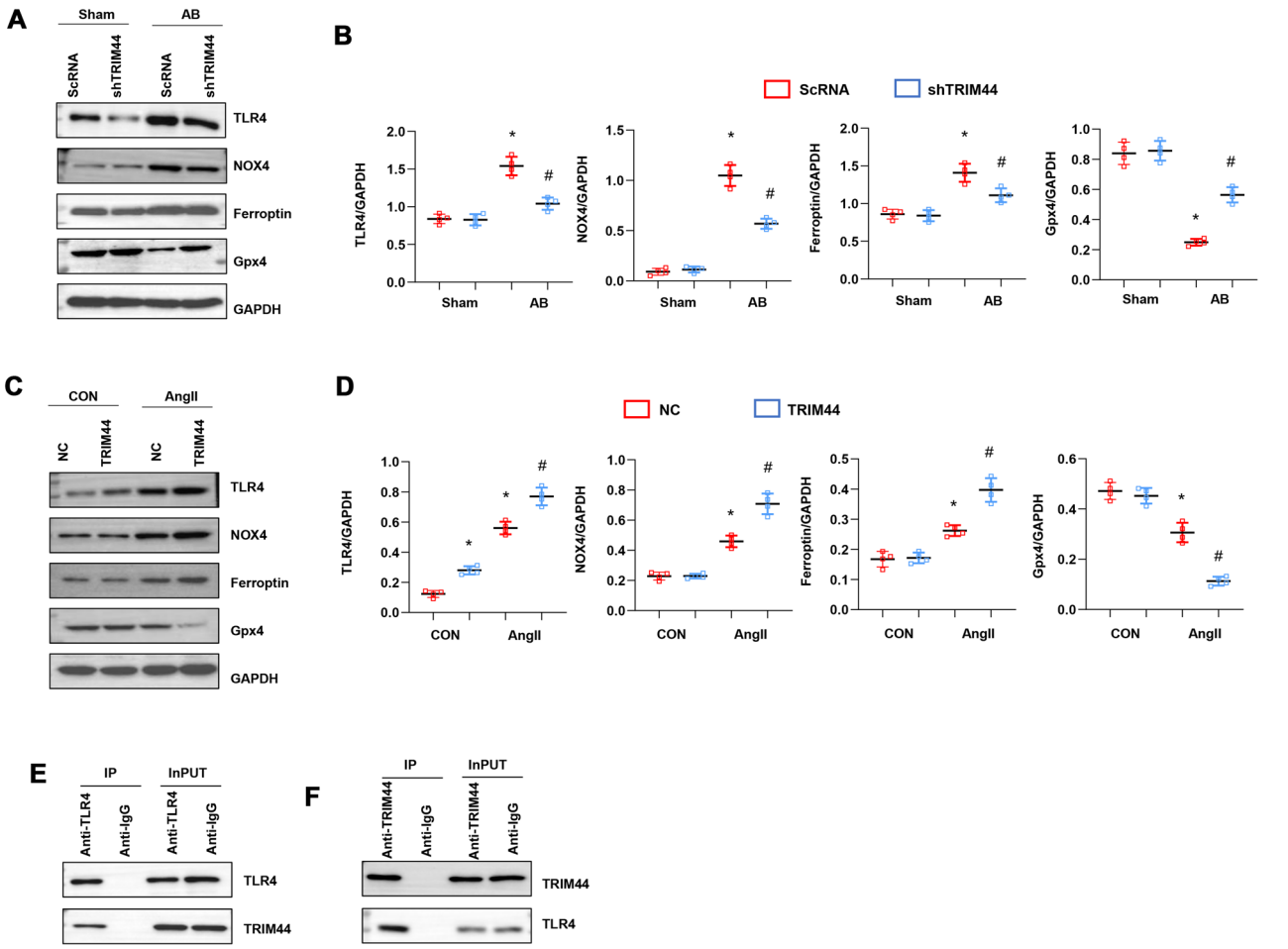

Fig. 8 TRIM44 interaction with TLR4 affected NOX4 signaling. **A**, **B** Protein levels of TLR4, NOX4, Gpx4, and ferritin in AAV-TRIM44 mice hearts 4 weeks post-AB ($n=4$). *$p<0.05$ vs. AAV-NC/sham group. #$p<0.05$ vs. AAV-NC/AB group. **C**, **D** Protein levels of TLR4, NOX4, Gpx4, and ferritin in TRIM44 siRNA-transfected H9c2 cells with Ang II challenge ($n=4$). *$p<0.05$ vs. scRNA/CON group. #$p<0.05$ vs. scRNA/Ang II group. **E**, **F** Co-IP assays of TLR4 and TRIM44 in cardiomyocytes

the ferroptosis inhibition protein GPX4 was reduced in mice hearts post-AB. TRIM44 KO increased the level of GPX4 and reduced the level of ferroportin. In cardiomyocytes, the level of ferroportin was increased post-Ang II stimulation (Fig. 8C and D). Likewise, the level of GPX4 in cardiomyocytes was reduced post-Ang II stimulation. TRIM44 overexpression decreased the level of GPX4 and increased the level of ferroportin. NOS, an oxidase that produces ROS and lipid ROS, was upregulated in both mice hearts post-AB and cardiomyocytes post-Ang II stimulation (Fig. 8A–D). NOX4 was reduced by TRIM44 KO in vivo (Fig. 8A and B) and increased in cardiomyocytes with TRIM44 overexpression (Fig. 8C and D). Previous studies found that TRIM44 could affect TLR4 stabilization. In this study, TLR4 expression was upregulated in both mice hearts post-AB and cardiomyocytes post-Ang II stimulation (Fig. 8A–D). Moreover, TLR4 was reduced by TRIM44 KO in vivo (Fig. 8A and B), but TLR4 was increased in cardiomyocytes with TRIM44 overexpression (Fig. 8C and D). The co-IP assay validated that TLR4 interacted with TRIM44 in cardiomyocytes (Fig. 8E and F).

TLR4 KO inhibited the effects of TRIM44 overexpression in mice

TLR4 KO mice were used to confirm that TLR4 is a target of TRIM44. The TLR4 protein was not detected in the heart tissue of TLR4-KO mice (Fig. 9A). TLR9-KO ameliorated pressure overload-induced cardiac hypertrophy, cardiac dysfunction, and fibrosis, which was evident from the histological analysis, echocardiography results, and fibrosis markers (Fig. 9B–I). Moreover, TRIM44 overexpression in TLR4-KO mice also improved cardiac hypertrophy, cardiac dysfunction, and fibrosis after 4 weeks in the AB model as compared to the WT-AB group (Fig. 9B–H). Taken together, TLR4 could be a target of TRIM44 in cardiac hypertrophy.

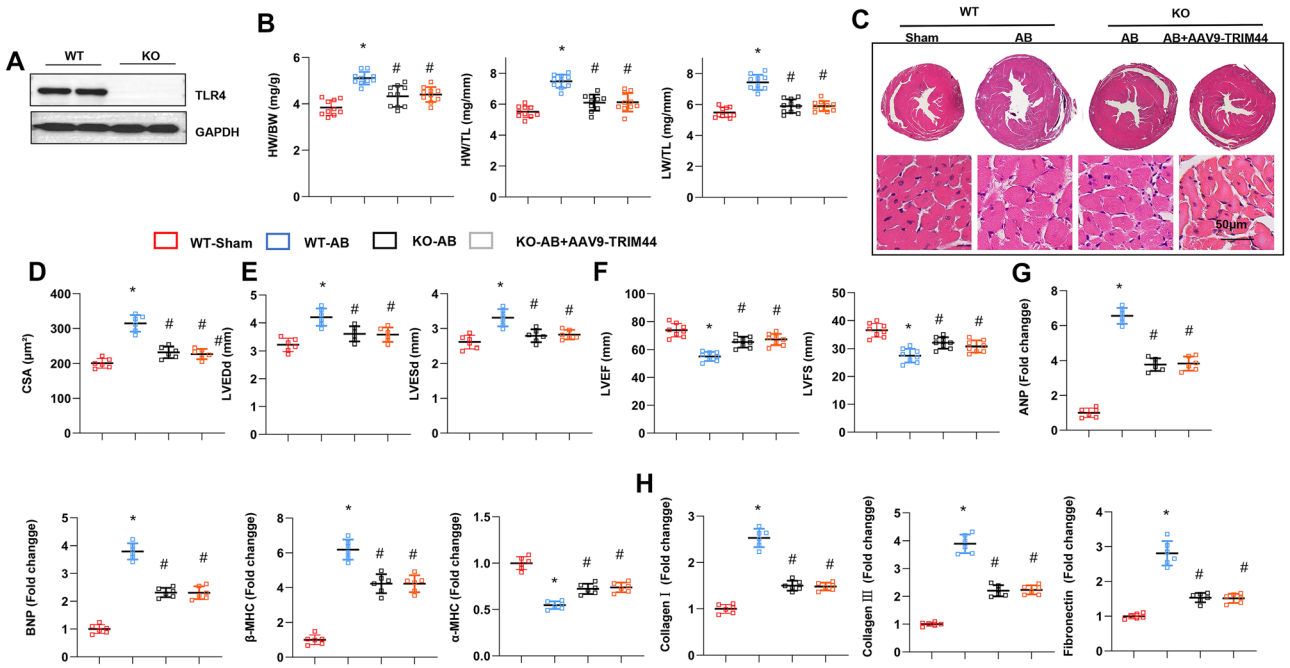

Fig. 9 TLR4 KO inhibited the effects of TRIM44 overexpression in mice. TLR4-KO mice were subjected to AAV9-TRIM44 injection in the AB model. **A** Protein level of TLR4 in TLR4-KO mice ($n=4$). **B**. HW/BW, HW/TL, and LW/BW in mice hearts 4 weeks post-AB ($n=8$). **C**, **D** H&E staining of mice hearts 4 weeks post-AB ($n=6$). **E**, **F** Echocardiography results in each group ($n=8$). **G**, **H** mRNA levels of pro-hypertrophy and fibrosis markers in heart tissue 4 weeks post-AB ($n=6$). *$p<0.05$ vs. WT/sham group. #$p<0.05$ vs. WT/AB group

Discussion

Pathological myocardial hypertrophy essentially transforms many cardiovascular diseases into heart failure [4]. At present, many mechanisms have been proposed, including the reduction of capillary density caused by myocardial hypertrophy, oxidative stress of cardiomyocytes, intracellular Ca^{2+} overload, apoptosis, and inflammatory reactions [2]. Jiang et al. found that TRIM44 KO attenuated isoproterenol-induced pathological cardiac remodeling [13]. In this study, it was demonstrated for the first time that TRIM44 expression was upregulated in pressure overload-induced adverse cardiac hypertrophy and cardiomyocytes with Ang II stimulation. Furthermore, TRIM44 overexpression in the heart aggravated cardiac hypertrophy, fibrosis, dysfunction, and lipid peroxidation. In contrast, TRIM44 KO ameliorated pressure overload-induced adverse cardiac hypertrophy, fibrosis, lipid peroxidation, and cardiac dysfunction. Thus, TRIM44 could be a therapeutic target for the prevention and treatment of cardiac hypertrophy.

TRIM44 is unique among the TRIM family proteins. The N-terminal of the TRIM44 protein contains a zinc finger ubiquitin protease domain (ZF-UBP), which functions as a deubiquitinase [9]. Studies have found that TRIM44 is upregulated in a variety of human tumors such as ovarian cancer, breast cancer, hepatocellular carcinoma, esophageal squamous cell carcinoma, and hepatocellular carcinoma [10, 14]. In this study, TRIM44 increased cardiomyocyte lipid peroxidation causing ferroptosis. Results also indicated that TRIM44 enhanced pressure overload-induced ferroptosis. Likewise, TRIM44 silencing reduced ferroptosis in vivo and in vitro. Ferroptosis is a form of cell death closely related to iron metabolism, which is characterized by the accumulation of lipid peroxidation, leading to the accumulation of lethal ROS [15]. Ferroptosis is manifested by the reduction of mitochondrial membrane density and the rupture of the mitochondrial outer membrane [15]. Upregulation of ER stress and inhibition of cystine/glutamate antiporter have been found to induce ferroptosis [16]. GPX4, heat shock protein β-1, and nuclear factor-erythroid 2-related factor 2 can negatively regulate ferroptosis by inhibiting the production of ROS and reducing cellular iron uptake. However, NADPH oxidase and p53 can positively regulate ferroptosis by promoting the production of ROS and inhibiting the expression of specific light chain subunit (SLC7A11) of cystine/glutamate antiporter [16]. Dysfunctional ferroptosis is closely related to cardiovascular diseases, such as myocardial ischemia–reperfusion injury, sepsis, myocardial injury, heart failure, and myocardial hypertrophy [17–19]. The findings of this study indicated the involvement of TRIM44 in ferroptosis and adverse cardiac hypertrophy.

NOX is a family of enzymes that generate ROS [35]. In mammals, NOX comprises multiple isoforms, namely, NOX1, NOX2, NOX3, NOX4, NOX5, dioxygenase (DUOX) 1, and DUOX2 [20]. Members of this family catalyze the reduction of oxygen to superoxide by using NADPH as an electron donor. In the heart, NOX4 is the predominant isoform in cardiomyocytes [21]. Elevation of NOX4 induces oxidative stress and ferroptosis in many diseases [22, 23]. In this study, NOX4 was upregulated in pressure-overloaded heart tissues and Ang II stimulated cardiomyocytes. Furthermore, TRIM44 could further increase the level of NOX4 level both in vivo and in vitro, while TRIM44 silencing reduced the expression of NOX4 protein level. Thus, TRIM44 may regulate ferroptosis by targeting NOX4 expression. The expression of TLR4 was also upregulated in TRIM44 transgenic mice hearts and cardiomyocytes. TLR4 is a pathogen-related and injury-related pattern recognition receptor, which is expressed on the myocardial cell membrane [24]. Biomolecules released by bacteria and injured cells can activate TLR4, which promotes downstream inflammation and injury response [24]. Recent studies have found that TLR4 can regulate NOX [23, 25]. In many disease models, NOX4 can interact with TLR4, which plays a big role in renal tubular epithelial cell damage, cerebral ischemic disease, and heart failure [23, 25]. An earlier study found that TRIM44 could directly bind and stabilize TLR4, causing melanoma progression [14]. Jiang et al. reported that TRIM44 KO ameliorated isoproterenol-induced rat cardiac remodeling by regulating the AKT/mTOR pathway. In this study, TRIM44 interacted with TLR4 and increased the level of TLR4 in the heart under adverse cardiac hypertrophy. Moreover, TLR4 KO could counteract the inhibitory effects of TRIM44 overexpression in vivo. This inconsistency might be due to some factors such as the different animal models and delivery systems used.

Taken together, TRIM44 aggravated pressure overload-induced cardiac hypertrophy via increased TLR4/NOX4-associated ferroptosis. Thus, TRIM44 may be a therapeutic target for the prevention and treatment of cardiac hypertrophy.

Author contribution Lu Gao and Yanzhou Zhang contributed to the conception and design of the experiments; Lu Gao, Leiming Wu, Lili Xiao, and Rui Yao carried out the experiments; Lili Xiao, Leiming Wu, and Zheng Wang analyzed the experimental results. Rui Yao wrote and revised the manuscript.

Funding This research was supported by the Henan Science and Technology Tackling Plan—Joint Construction Project [No. LHGJ20190100].

Availability of data and materials The datasets used and/or analyzed during the current study are available from the corresponding author on reasonable request.

Declarations

Ethical approval The animal experiments were performed according to the Guide for the Care and Use of Laboratory Animals published by the US National Institutes of Health (NIH Publication No. 85–23, revised 1996) and were approved by the Animal Care and Use Committee of the First Affiliated Hospital of Zhengzhou University (ZH-2021–0120).

Consent to participate Not applicable.

Competing interest The authors declare no competing interests.

References

1. Yang D, Liu HQ, Liu FY, Guo Z, An P, Wang MY, Yang Z, Fan D, Tang QZ (2021) Mitochondria in Pathological cardiac hypertrophy research and therapy. Front Cardiovasc Med 8:822969
2. Nakamura M, Sadoshima J (2018) Mechanisms of physiological and pathological cardiac hypertrophy. Nat Rev Cardiol 15:387–407
3. Zhu L, Li C, Liu Q, Xu W, Zhou X (2019) Molecular biomarkers in cardiac hypertrophy. J Cell Mol Med 23:1671–1677
4. Lyon RC, Zanella F, Omens JH, Sheikh F (2015) Mechanotransduction in cardiac hypertrophy and failure. Circ Res 116:1462–1476
5. Matsuura TR, Leone TC, Kelly DP (2020) Fueling cardiac hypertrophy. Circ Res 126:197–199
6. Liu J, Li W, Deng KQ, Tian S, Liu H, Shi H, Fang Q, Liu Z, Chen Z, Tian T et al (2022) The E3 ligase TRIM16 is a key suppressor of pathological cardiac hypertrophy. Circ Res 130:1586–1600
7. Sparrer KMJ, Gableske S, Zurenski MA, Parker ZM, Full F, Baumgart GJ, Kato J, Pacheco-Rodriguez G, Liang C, Pornillos O et al (2017) TRIM23 mediates virus-induced autophagy via activation of TBK1. Nat Microbiol 2:1543–1557
8. Li Y, Meng Q, Wang L, Cui Y (2021) TRIM27 protects against cardiac ischemia-reperfusion injury by suppression of apoptosis and inflammation via negatively regulating p53. Biochem Biophys Res Commun 557:127–134
9. Lyu L, Chen Z, McCarty N (2022) TRIM44 links the UPS to SQSTM1/p62-dependent aggrephagy and removing misfolded proteins. Autophagy 18:783–798
10. Yu XZ, Yuan JL, Ye H, Yi K, Qie MR, Hou MM (2021) TRIM44 facilitates ovarian cancer proliferation, migration, and invasion by inhibiting FRK. Neoplasma 68:751–759
11. Luo F, Wu Y, Zhu L, Zhang J, Liu Y, Jia W (2020) Knockdown of HIF1A-AS2 suppresses TRIM44 to protect cardiomyocytes against hypoxia-induced injury. Cell Biol Int 44:1523–1534
12. Gao L, Liu Y, Guo S, Xiao L, Wu L, Wang Z, Liang C, Yao R, Zhang Y (2018) LAZ3 protects cardiac remodeling in diabetic cardiomyopathy via regulating miR-21/PPARa signaling. Biochim Biophys Acta Mol Basis Dis 1864:3322–3338
13. Jiang XY, Guan FF, Ma JX, Dong W, Qi XL, Zhang X, Chen W, Gao S, Gao X, Pan S et al (2023) Cardiac-specific Trim44 knockout in rat attenuates isoproterenol-induced cardiac remodeling via inhibition of AKT/mTOR pathway. Dis Model Mech 16
14. Wei CY, Wang L, Zhu MX, Deng XY, Wang DH, Zhang SM, Ying JH, Yuan X, Wang Q, Xuan TF et al (2019) TRIM44 activates the AKT/mTOR signal pathway to induce melanoma progression by stabilizing TLR4. J Exp Clin Cancer Res 38:137
15. Xie Y, Hou W, Song X, Yu Y, Huang J, Sun X, Kang R, Tang D (2016) Ferroptosis: process and function. Cell Death Differ 23:369–379

16. Li N, Jiang W, Wang W, Xiong R, Wu X, Geng Q (2021) Ferroptosis and its emerging roles in cardiovascular diseases. Pharmacol Res 166:105466
17. Fang X, Wang H, Han D, Xie E, Yang X, Wei J, Gu S, Gao F, Zhu N, Yin X et al (2019) Ferroptosis as a target for protection against cardiomyopathy. Proc Natl Acad Sci U S A 116:2672–2680
18. Li N, Wang W, Zhou H, Wu Q, Duan M, Liu C, Wu H, Deng W, Shen D, Tang Q (2020) Ferritinophagy-mediated ferroptosis is involved in sepsis-induced cardiac injury. Free Radic Biol Med 160:303–318
19. Wang J, Deng B, Liu Q, Huang Y, Chen W, Li J, Zhou Z, Zhang L, Liang B, He J et al (2020) Pyroptosis and ferroptosis induced by mixed lineage kinase 3 (MLK3) signaling in cardiomyocytes are essential for myocardial fibrosis in response to pressure overload. Cell Death Dis 11:574
20. Bedard K, Krause KH (2007) The NOX family of ROS-generating NADPH oxidases: physiology and pathophysiology. Physiol Rev 87:245–313
21. Cadenas S (2018) ROS and redox signaling in myocardial ischemia-reperfusion injury and cardioprotection. Free Radic Biol Med 117:76–89
22. Park MW, Cha HW, Kim J, Kim JH, Yang H, Yoon S, Boonpraman N, Yi SS, Yoo ID, Moon JS (2021) NOX4 promotes ferroptosis of astrocytes by oxidative stress-induced lipid peroxidation via the impairment of mitochondrial metabolism in Alzheimer's diseases. Redox Biol 41:101947
23. Chen X, Xu S, Zhao CLiu B (2019) Role of TLR4/NADPH oxidase 4 pathway in promoting cell death through autophagy and ferroptosis during heart failure. Biochem Biophys Res Commun 516:37–43
24. de Vicente LG, Munoz VR, Pinto AP, Rovina RL, da Rocha AL, Marafon BB, Tavares MEA, Teixeira GR, Ferrari GD, Alberici LC et al (2021) TLR4 deletion increases basal energy expenditure and attenuates heart apoptosis and ER stress but mitigates the training-induced cardiac function and performance improvement. Life Sci 285:119988
25. Suzuki Y, Hattori K, Hamanaka J, Murase T, Egashira Y, Mishiro K, Ishiguro M, Tsuruma K, Hirose Y, Tanaka H et al (2012) Pharmacological inhibition of TLR4-NOX4 signal protects against neuronal death in transient focal ischemia. Sci Rep 2:896